Published in final edited form as:
*J Mater Chem*. 2012 October 7; 22(37): 19429–19437. doi:10.1039/C2JM31768K.

# Photoreactive elastin-like proteins for use as versatile bioactive materials and surface coatings

**Jordan Raphel**[a], **Andreina Parisi-Amon**[b], and **Sarah Heilshorn**[a]

[a]Department of Materials Science & Engineering, Stanford University. 476 Lomita Mall, McCullough Building 246, Stanford, CA 94035, USA

[b]Department of Bioengineering, Stanford University, Stanford, CA, USA

## Abstract

Photocrosslinkable, protein-engineered biomaterials combine a rapid, controllable, cytocompatible crosslinking method with a modular design strategy to create a new family of bioactive materials. These materials have a wide range of biomedical applications, including the development of bioactive implant coatings, drug delivery vehicles, and tissue engineering scaffolds. We present the successful functionalization of a bioactive elastin-like protein with photoreactive diazirine moieties. Scalable synthesis is achieved using a standard recombinant protein expression host followed by site-specific modification of lysine residues with a heterobifunctional N-hydroxysuccinimide ester-diazirine crosslinker. The resulting biomaterial is demonstrated to be processable by spin coating, drop casting, soft lithographic patterning, and mold casting to fabricate a variety of two- and three-dimensional photocrosslinked biomaterials with length scales spanning the nanometer to millimeter range. Protein thin films proved to be highly stable over a three-week period. Cell-adhesive functional domains incorporated into the engineered protein materials were shown to remain active post-photo-processing. Human adipose-derived stem cells achieved faster rates of cell adhesion and larger spread areas on thin films of the engineered protein compared to control substrates. The ease and scalability of material production, processing versatility, and modular bioactive functionality make this recombinantly engineered protein an ideal candidate for the development of novel biomaterial coatings, films, and scaffolds.

## Introduction

Protein thin films are widely employed components in many biomedical systems. For example, cell-adhesive proteins films that are able to coat synthetic implants, thereby presenting a more favorable surface for *in vivo* interactions, have found applications in nerve guides[1], bone grafts[2], and vascular grafts[3]. Commonly, these coatings are made from adsorbed layers of native extracellular matrix (ECM) proteins including collagen[4, 5], laminin[5, 6], and fibronectin[5] among others. While the appeal of using naturally derived materials for *in vivo* applications is clear, there are certain key limitations affecting the efficacy of these systems. When selecting naturally derived materials, one is limited to those materials that can be harvested and purified sufficiently so as to not cause immunogenic responses post implantation.[8] Furthermore, although bioactive, these materials suffer from significant batch-to-batch variations in their mechanical and biochemical properties, leading to irreproducible coating performance, especially on larger scales.[9] In addition, these films



Fax: 650-498-3763; Tel:650-723-3763; heilshorn@stanford.edu.

Electronic Supplementary Information (ESI) available: See DOI: 10.1039/b000000x/

are often adsorbed coatings, which can cause irregularities in thickness and density, and hence bioactivity.

Engineered proteins harness the bioactive functionality of naturally derived materials, while overcoming their limitations through highly reproducible and modular chemical compositions, making them ideal for many biomedical applications.[10–13] The modular design strategy employed in the creation of engineered proteins allows for the inclusion of multiple peptide domains with distinct functionalities into one surface coating material. Exploration of tissue development and regeneration has led to the discovery of a multitude of cell-instructive peptide domains that can be included in an engineered protein sequence. In addition, these domains are incorporated in a regulated manner, allowing for independent control of material properties such as ligand density, material degradation rate, and mechanical properties.[14, 15]

These protein-engineered biomaterials are synthesized by utilizing the machinery of living cells to translate a recombinant plasmid that encodes the desired amino acid sequence.[16] Because the exact protein sequence is specified and reliably produced through recombinant methods, these materials offer exquisite control over the resulting material properties.[14] In addition to the inclusion of bioactive and cell-instructive peptide domains, specific individual amino acids can be incorporated at defined locations to confer easy chemical modifications. For example, cysteine residues are often employed for straightforward thiol reactions[13, 17], while lysine residues are targeted for primary amine chemistries[18]. These sites are frequently used to attach other molecules such as drugs to yield bioactive protein-conjugates[19] or to react with homofunctional crosslinking molecules to form bulk biomaterials. Common homofunctional, primary amine-reactive crosslinkers include diisocyanates[20], propionic acids[21], and N-hydroxysuccinimide esters[22]. However, these homofunctional crosslinkers are not without their own limitations, such as the potential cytotoxicity of the crosslinking reagents and their residual reaction byproducts. Additionally, crosslink formation can begin as soon as the crosslinker is added, with reaction kinetics often on the same time scale as the mixing process, potentially resulting in inhomogeneities at the cellular length scale.

Photocrosslinking is a processing method commonly used to overcomes these concerns in the production of a variety of biomedical polymeric materials.[23] This technique confers the ability to easily pattern polymer structures, which have far-ranging applications including the development of drug delivery vehicles, implant coatings, and tissue engineering scaffolds.[24, 25] Photocrosslinking also enables fast processing, as these reactions are often quite rapid.[26] Furthermore, the use of focused light sources and photomasks facilitates exquisite spatial and temporal control of crosslinking reactions.[27] Importantly, many photoreactions have been proven cytocompatible, enabling direct photo-encapsulation of cells.[24] While photoreactions are a common strategy for processing synthetic polymers, proteins are not inherently photoactive, making the addition of photoactive functionality to protein-based biomaterials an important target.

Previous work has demonstrated the usefulness of photoreactive, protein-engineered biomaterials to create cell-adhesive, lithographically patterned substrates. Photoreactivity was conferred on the protein through the incorporation of a non-canonical, photoreactive amino acid directly into the protein sequence.[28–30] While solid phase synthesis of peptides can easily accommodate non-canonical amino acids, this technique is limited to chains of about 70 amino acids or less.[31] Synthesis of longer proteins that contain non-canonical amino acids can be achieved through genetic engineering of auxotrophic bacterial hosts, i.e. organisms incapable of synthesizing a specific amino acid, which is then replaced by a non-canonical analog.[28, 29, 32] Carrico, et al. used this strategy to effectively synthesize

photocrosslinkable elastin-like protein (ELP) materials using the non-canonical amino acid *para*-azidophenylalanine.[29] This ELP also included a cell-adhesive RGD peptide domain that was shown to retain its bioactivity after photocrosslinking was initiated by irradiation with ultraviolet wavelength light.[29] This work serves as an elegant proof of concept that photocrosslinkable ELPs can be engineered while retaining relevant bioactive functionalities. However, protein yields using genetically engineered auxotrophic microorganisms are typically quite low, limiting the scalability and wide spread application of this approach.

As an alternative strategy, we demonstrate synthesis of an engineered ELP in a commercially available *Escherichia coli* strain optimized for recombinant protein yield followed by post-processing to append photoreactive moieties onto the protein backbone. Our ELP is a previously reported block copolymer designed to contain four repeats of an elastin-like structural domain and a bioactive, cell-adhesive domain incorporating the extended fibronectin RGD sequence (Figure 1).[14] A heterobifunctional N-hydroxysuccinimide ester-diazirine (NHS-diazirine, succinimidyl 4,4'-azipentanoate) is conjugated to the ELP via reaction with the primary amine side chains of the canonical lysine amino acid residues. Chemical modification of the engineered protein post-expression enables synthesis of a photoactive protein material while simultaneously utilizing the inherent scalability of recombinant protein expression.

We demonstrate the potential applications of this technique through synthesis of a reliable, versatile, scalable ELP biomaterial that can be photo-processed in multiple ways. Two-dimensional (2D) protein coatings are produced by spin coating and drop casting, while bulk, three-dimensional (3D) scaffolds are formed by mold casting. The coating and crosslinking procedures are reliable and straightforward, producing materials that retain their cell-adhesive biofunctionality to interact with human adipose-derived stem cells (hASCs), a clinically important cell type. hASCs are primary mesoderm cells isolated from adult tissue that can differentiate along any of the mesodermal lineages. These cells are accessible in high numbers from consenting adult donors, circumventing ethical issues often attributed to other stem cell therapies. Furthermore, these cells demonstrate enhanced reprogramming efficiency to become induced pluripotent stem cells, thereby enabling differentiation into cell types of other lineages.[33] Transplantation of hASCs holds tremendous potential in the development of future regenerative medicine therapies.[34, 35] Taken together, the bioactivity of this photocrosslinkable ELP material to promote hASC adhesion, along with its versatility to produce coatings, thin films, and bulk scaffolds, encourage further development for applications in implant coatings and tissue engineering scaffolds.

## Experimental

### Recombinant Synthesis and Purification of ELP

ELP and scrambled-ELP (a negative control protein containing a non-cell-adhesive sequence, Figure S1) were expressed and purified as previously reported.[14] Briefly, a plasmid encoding the protein sequence was transformed into an *Escherichia coli* host (BL21(DE3), NEB) and expression was induced under control of the T7-lac promoter. After cell lysis, the target protein was purified by repeated centrifugation at alternating temperatures (4 °C and 37 °C), utilizing the lower critical solution temperature of the ELP. Protein purity was assessed by gel electrophoresis. ELP was dialyzed, lyophilized, and stored at room temperature.

### ELP-diazirine Conjugation

A heterobifunctional N-hydroxysuccinimide ester-diazirine crosslinker, (NHS-diazirine, succinimidyl 4,4'-azipentanoate, Pierce Biotechnology) was dissolved in dimethyl sulfoxide and mixed with a solution of ELP, dissolved in either 20 mM HEPES or phosphate buffered saline (PBS). After reaction, the diazirine-conjugated ELP (ELP-D) was dialyzed against DI $H_2O$ for 48 hours, frozen, and lyophilized. The conjugation efficiency was determined by 2,4,6-trinitrobenzene sulfonic acid (TNBSA, Pierce Biotechnology) assay to detect unreacted primary amines. Briefly, a solution of protein in PBS was diluted in sodium bicarbonate buffer followed by the addition of TNBSA reagent. After two hours of incubation at room temperature, the reaction was stopped with a combination of sodium dodecyl sulfate and hydrochloric acid, and the absorbance at 335 nm was taken for comparison to a standard curve of non-conjugated ELP.

### Photocrosslinking of ELP-D Materials

ELP was resuspended from a lyophilized state in PBS at 4 °C. All protein materials were made using 50 mg/mL (5 wt%) solutions. Protein films were fabricated by spin coating protein solution onto 12-mm glass coverslips (Fisher). Coverslips, previously rinsed in ethanol, dried with nitrogen gas, and stored at 4 °C for a minimum of 1 hour prior to use, were placed on the stage of a spin coater (WS-400-6NPP, Laurell Technologies). The protein solution (14 μL) was placed onto the center of the coverslip and spun at various speeds (4,000 – 8,000 rpm) for 90 seconds. Drop casted films were made by spreading protein solution on the substrate of interest with a pipette tip. Bulk protein scaffolds were made by adding protein solution (40 μL) to a 10-mm tall, 4.5-mm diameter circular mold. Patterned scaffolds were made via soft lithography by adding protein solution to a stripe-patterned (50 μm width, 5 μm depth) poly(dimethyl siloxane) (PDMS) mold. The solution-filled mold was covered by a glass coverslip and allowed to dry overnight at 37 °C. After processing, all materials were exposed to ultraviolet light using a 365 nm, 8 watt light source (3UV-38, UVP). Spin coated films and PDMS patterned scaffolds were exposed for 1 hour at an exposure distance of 3 cm, while drop cast films and bulk scaffolds were exposed for 2 hours at the same conditions.

### Scanning Electron Microscopy (SEM) Characterization

SEM samples were spin coated using the protocol above, 4,000 rpm for 90 seconds. Film morphology samples were left hydrated without any further processing and imaged via variable-pressure SEM (Hitachi S-3400N Variable Pressure SEM, operated at 15 kV, pressure 50–60 Pa, using a Deben Coolstage for temperature control). Film thickness samples were air dried, sputter coated with a layer of gold, and imaged via field emission SEM (FEI Magellan 400 XHR, operated at 5 kV).

### Fourier Transform Infrared Spectroscopy (FTIR) Characterization

Protein films were spin coated on 13-mm diameter zinc selenide discs (Perkin Elmer) using an identical procedure as for the glass coverslips given above. Measurements were performed using an FTIR spectrometer (Vertex 70, Bruker Optics), purged with nitrogen gas. A non-coated zinc selenide disc was used for background control. The films were exposed to the 365 nm light source described above for varying amounts of time, with an FTIR measurement after each exposure time. A single measurement consisted of 200 scans with a resolution of 4 $cm^{-1}$. Disappearance of the characteristic diazirine peak (1460 $cm^{-1}$) upon photoactivation was reported as total peak area over time.

### Mechanical Properties Characterization

Uniaxial tensile tests were performed on drop cast, crosslinked ELP-D films using a mechanical testing system (Bionix 200, MTS Systems Corporation). A 44.48-N load cell was used to characterize the force-displacement curve, which was converted to engineering stress and strain using the initial dimensions of the ELP-D films. The Young's modulus is the slope of the linear portion of the engineering stress-strain curve.

### Thin Film Mass Characterization

The mass of protein in spin coated films was determined by a bicinchoninic acid (BCA) endpoint assay (QuantiPro, Sigma Aldrich). Briefly, protein films for each time point (n=4) were submerged in 500 μL PBS, followed by the addition of 500 μL of BCA reagent (25:25:1 QA buffer:QB buffer:copper II sulfate solution). The reaction was incubated at 60 °C for 1 hour, equilibrated at room temperature for 20 minutes, and quantified by absorbance at 562 nm for comparison to a standard curve.

### hASC Isolation and *in vitro* Culture Maintenance

ASCs were isolated from human lipoaspirate from the flank and thigh regions by suction assisted liposuction. All subjects donating tissue for this research responded to an Informed Consent, which has been approved by the Stanford Institutional Review Board. Specimens were washed in dilute betadine, rinsed twice in PBS, and digested with 0.075% Type II collagenase in Hank's Balanced Salt Solution at 37 °C under agitation for 30 minutes. Next, collagenase was inactivated by an equal volume of PBS with 10% fetal bovine serum (FBS) and 100 IU/ml penicillin/streptomycin. The stromal vascular fraction was then pelleted, resuspended, and filtered through a 100-μm strainer before being plated into a 100-mm dish. Adherent cells were cultured in DMEM supplemented with 10% FBS and 100 IU/ml penicillin/streptomycin at 37 °C and 5% atmospheric $CO_2$. Cells were expanded and passaged by trypsinization for subsequent use in *in vitro* assays.

### hASC Culture on Photocrosslinked ELP-D Thin Films

Cells were seeded at $1.24\times10^4$ cells/$cm^2$ onto spin coated thin films of ELP-diazirine (ELP-D), scrambled-ELP-D, or non-coated 12-mm glass coverslips (Fisher) (n=4 independent samples for each condition). Phase contrast images were taken at 2, 3, 4, 5, and 6 hours post-seeding using an inverted light microscope (Zeiss Axiovert) at four random positions for each substrate. Individual cells were scored as either adherent (i.e., appearing dark by phase contrast) or non-adherent (i.e., appearing refractile by phase contrast). Statistical significance was analyzed using the Kruskal-Wallis 1-way ANOVA. At six days, cell viability was assessed with a fluorescent LIVE/DEAD® cytotoxicity kit (Molecular Probes, 2.0 μM calcein AM and 4.0 μM ethidium homodimer). Other cultures were fixed overnight in 4% paraformaldehyde and blocked with 10% normal goat serum or FBS containing 0.1% v/v Triton X-100 in PBS for one hour at room temperature. After rinsing, samples were stained with 6-diamidino-2-phenylindole (DAPI, 2 μg/ml, Roche) to visualize cell nuclei and with rhodamine-conjugated phalloidin (1:200 dilution, Invitrogen) to visualize F-actin. Fluorescent images were obtained with a confocal microscope (Leica SPE) and manually analyzed with ImageJ software (NIH) to determine spread cell area (n = 37 – 83 cells per condition). Statistical significance was determined using the Mann Whitney t test. At day six, alamarBlue® assay (Invitrogen) was used to assess metabolic activity. Briefly, alamarBlue reagent was added to the cells (50 μM), incubated at 37 °C for 2 hours, and analyzed for fluorescence signal (n = 3 independent samples for each condition). Statistical significance was determined using the Mann Whitney t test.

## Results and Discussion

### Engineered Protein Synthesis and Conjugation with Photoreactive Moieties

ELP was synthesized via recombinant expression from a commercially available *Escherichia coli* host and purified by utilizing the material's lower critical solution temperature (LCST) as previously described.[14] As with other reported elastin-like variants with the repetitive VPGXG amino acid sequence (where X is any amino acid), this engineered ELP is soluble in aqueous solutions below the LCST and forms a polymer-rich coacervate above this temperature.[36] Therefore, engineered ELPs comprised of canonical amino acids can be synthesized and purified using protocols that are easily scalable.[37] The elastin-like repetitive sequence was modified to include one lysine residue per five VPGXG repeats to enable site-specific, post-purification reactivity via primary amine-based chemistry (full amino acid sequence given in Fig. S1).[22] The purified ELP was covalently conjugated with a heterobifunctional NHS-diazirine photocrosslinker (succinimidyl 4,4'-azipentanoate), resulting in ELP-diazirine (ELP-D). The diazirine moiety is activated upon exposure to long wavelength ultraviolet light (330–370 nm), releasing $N_2$ and forming a highly reactive carbene intermediate that can rapidly insert into neighboring protein chains at any amino acid site (Fig. 1A).[38]

The conjugation efficiency of the NHS-diazirine to the ELP was determined by quantifying the number of unreacted primary amines post-reaction. Three reaction times (6, 15, and 24 hours) and four reaction stoichiometries (0.25, 0.5, 1.0, and 2.0 moles of crosslinker per mole of primary amines contained within the ELP) were assessed. As expected, the conjugation efficiency was directly related to the stoichiometric ratio of crosslinker to primary amines (Fig. 1B). A reaction time of 6 hours was found to be sufficient, as further increasing the reaction time did not improve the conjugation efficiency (data not shown). After 6 hours, a range of 9.96% to 90.3% of primary amines were reacted, corresponding to an average of 1.4 to 12.6 diazirines attached per protein chain. Having reliable control over the conjugation efficiency, and hence the maximum number of potential crosslinks formed per protein chain, enables direct tuning of the final biomaterial crosslinking density. In addition, having reliable control over the number of unmodified lysine residues enables potential future use of the remaining primary amine side chains as grafting sites for growth factor or drug conjugation. Further experiments for this manuscript utilized a stoichiometric ratio of 1:1 crosslinker:primary amine (58.5% conjugation efficiency) to demonstrate stable biomaterial formation even when ~40% of lysine residues are unmodified.

The photoactivation kinetics of the diazirine moiety on ELP-D were examined using Fourier transform infrared spectroscopy (FTIR) by monitoring the peak intensity area of the diazirine $\nu 3$ fundamental peak (1460 $cm^{-1}$) (Fig. 1C).[39] Photoactivation of diazirine releases $N_2$, which does not absorb infrared irradiation due to its symmetry. Therefore, an increase in transmittance (i.e., decrease in peak intensity area) at the characteristic diazirine peak is directly correlated with the formation of a photoactivated moiety. The photoactivation followed first-order reaction kinetics with an exponential decay in diazirine concentration and a diazirine half-life ($t_{1/2}$) of 119 seconds. This result corroborates the reported $t_{1/2}$ = 2 minutes for photoactivated diazirine.[40] These data suggest that the degree of diazirine activation, and hence the crosslinking concentration within ELP-D, can be directly controlled by varying the ultraviolet exposure time.

### Versatile Photo-Processing of ELP-D Films and Scaffolds

To demonstrate the versatility of ELP-D, several biomaterial processing techniques were employed to create stable 2D thin films and 3D scaffolds. First, ELP-D films were drop cast directly onto a hydrophobic surface such as Parafilm, dried in air, crosslinked by ultraviolet

light exposure, and then easily removed from the surface by peeling to create a free-standing film (Fig. 2A). A 10 mg film was measured to be 50 μm thick and was able to fully support a 4.5 g mass (Fig. 2B). Tensile tests were performed on these drop cast films in the dehydrated state. The Young's modulus of the dehydrated film was 250 MPa, and the film displayed little plasticity prior to fracture (Fig. 2C). These films verify the functionality of the photoreactive moiety to form a strong network of crosslinked protein, resulting in a solid, mechanically stable material. As drop casting results in films of variable thickness, we then explored the use of spin coating to create films of defined, uniform thickness.

As a second demonstration, spin coating of ELP-D onto glass coverslips followed by photocrosslinking resulted in uniform protein coatings as visualized by scanning electron microscopy (SEM, Fig. 2D). The retained protein mass, and hence thickness, of the films was controlled by altering the speed of the spin coating process (Fig. 2E). For a 70 μg film, which corresponds to 10% protein retention during the spin coating process at a spin speed of 6,000 rpm, the approximate thickness is estimated to be ~500 nm (assuming a density of ELP-D on the order of native elastin, 1.3 mg/cm$^3$). SEM of dried thin film cross-sections corroborated this estimation (Fig. S2). These thin films may be useful as resilient coatings on biomedical implants, where specific biofunctionality can be imparted to the implant surface through engineering of the modular engineered ELP.[41]

Bulk scaffolds were also made from the ELP-D biomaterial by crosslinking the protein solution within preformed molds. In the first example, a 5 wt% ELP-D solution was photocrosslinked to yield a swollen, cylindrical hydrogel 2 mm tall and 4.5 mm in diameter (Fig. 2F). This type of bulk, monolithic scaffold is well suited for use as a tissue engineering scaffold, and indeed, other ELP biomaterials have been explored as tissue engineering scaffolds for a wide variety of applications.[42]

As a second example, micropatterned topography was added to a bulk ELP-D scaffold using soft lithography techniques. A polydimethylsiloxane (PDMS) stamp with parallel grooves, 50 μm wide and 5 μm deep, was used as a templating substrate for an ELP-D solution containing fluorescently labeled ELP-D for visualization. The templated and photocrosslinked ELP-D formed a scaffold with uniform and regularly spaced channels, as visualized by fluorescence microscopy (Fig. 3A). Soft lithography processing could be used to create large-scale, bioactive, patterned structures, promising for use as cell-directive scaffolds for engineering tissues where specific cellular orientation and organization are critical to function, such as in vascular[43] and cardiac[44] tissues.

The use of such a wide range of processing techniques exemplifies the versatility and amenability of ELP-D for a variety of biomaterial and tissue engineering applications. Unlike previous work that was limited to thin film applications, the scalable synthesis, purification, and photo-processing techniques utilized here enable the formation of 2D and 3D scaffolds ranging in size scale from nanometers (Fig. 2D) to micrometers (Fig. 2A,B) to millimeters (Fig. 2F).

## Photocrosslinked ELP-D Biomaterial Stability

A series of experiments were performed to assess the short- and long-term stability of photocrosslinked ELP-D materials. First, to demonstrate the requirement of the diazirine moiety, both ELP and ELP-D scaffolds were micropatterned on PDMS soft lithography molds. Prior to ultraviolet light exposure, fluorescence microscopy revealed that both materials formed micropatterned surfaces with uniform grooves, although the raised ridges of ELP appeared slightly more swollen than ELP-D (Fig. 3A). Both patterned substrates were exposed to ultraviolet light for one hour followed by soaking in aqueous buffer for 24 hours. Further microscopy revealed that the ELP substrate was completely solubilized

during this time, while the ELP-D material was still present and retained the striped micropattern, exhibiting swollen but still uniform grooves (Fig. 3A).

Next, to demonstrate thin film stability, solutions of ELP and ELP-D were spin coated onto glass coverslips. The amount of engineered protein retained on each coverslip was quantified before and at various time points after ultraviolet light exposure and rinsing (Fig. 3B). The ELP and ELP-D thin films initially contained a similar amount of material (~19 μg, as shown by the no UV exposure and no rinsing condition). After ultraviolet light exposure and a four hour rinse, both films showed a loss of protein, with 38%±3.5% of ELP-D and 11%±4.7% of ELP retained on the coverslips. Over the subsequent week, protein retention on the ELP-coated coverslips was negligible, while no further protein was lost from the ELP-D thin films. The initial ELP-D protein loss at four hours is presumably due to solubilization of protein chains that were not effectively crosslinked into the polymer network. Once these non-crosslinked chains are removed, the remainder of the ELP-D thin film retained its stability for up to one week (the longest time point tested).

Next, we assessed the role of initial thin film mass in determining the long-term film stability and required rinsing time. Glass coverslips were spin coated with ELP-D at either 8000 or 4000 rpm, yielding thin films with masses of ~20 or ~40 μg, respectively (estimated thicknesses of 275 or 675 nm, respectively). These films were crosslinked by ultraviolet light exposure, and their protein retention was quantified over a three-week period of continuous rinsing (Fig. 3C). Both thin films experienced significant protein loss during the initial four hour rinse. After this time point, both films proved to be very stable, losing negligible amounts of protein over the subsequent 21 days. Therefore, a four hour rinse time is sufficient to fabricate stable ELP-D thin films regardless of initial film mass. In addition, this protocol was found to be a highly reproducible method to produce thin films of a specific final mass, as evidenced by the narrow standard deviation for both sets of films. Due to this, we can reliably alter the final quantity of protein retained on the coated surface, and thus the total concentration of presented bioactive ligand.

Stability is an integral parameter dictating potential biomedical applications. The high level of stability displayed by photocrosslinked ELP-D thin films makes them promising materials for use as implant coatings, which commonly need to remain intact over long periods of time. Stability within an *in vivo* setting remains to be evaluated. Native elastin is highly persistent in the body, although it can be rapidly degraded by the enzyme elastase.[45] Previous work with ELP materials has demonstrated that the proteolytic degradation rate can be tailored over two orders of magnitude by designing specific protease enzyme target sites into the amino acid sequence.[14] A similar strategy could be utilized with these ELP-D thin films to control the film degradation rate for potential drug delivery applications. Importantly, this high level of film stability was demonstrated for ELP-D conjugated at ~60% efficiency, leaving ~5 unreacted primary amines per protein chain. These reactive groups could be used to tether various drugs or growth factors into the ELP-D thin film. Alternatively, ELP-D conjugated with more crosslinker per protein chain could be used to decrease the initial protein loss, increasing the concentration of bioactive domains present on the coated surface.

### Photocrosslinked ELP-D Films Support hASC Culture

To demonstrate that the cell-adhesive, RGD bioactive domains retain functionality after photo-processing, human adipocyte-derived stem cells (hASCs) were seeded onto spin coated ELP-D thin films. For comparison, cells were seeded on non-coated glass as well as negative control thin films that were otherwise identical to ELP-D except they contained a non-cell-adhesive RDG peptide sequence (scrambled-ELP-D).[14] All experiments were performed in medium supplemented with 10% serum. During the six hours immediately

after seeding, a significantly larger percentage of hASCs were adherent on the ELP-D thin films compared to the scrambled-ELP-D surfaces, as manually quantified from phase contrast imaging (Fig. 4A).

To further investigate potential morphological differences between adherent cells on ELP-D and scrambled-ELP-D films, hASCs were fixed and fluorescently stained four hours after seeding. Individual cells were manually outlined, and cell spread areas were quantified using ImageJ software. Although the hASC population exhibited a wide, non-Gaussian distribution in spread area on both surfaces, the ELP-D films initiated significantly more spreading than the scrambled-ELP-D films (Fig. 4B). In addition, fluorescent micrographs of F-actin polymerized cytoskeletal fibers qualitatively corroborate these data (Fig. 4C).

Cytocompatibility of the ELP-D thin films was confirmed through a longer, six-day study. As expected, fluorescent stains for live (calcein AM) and dead (ethidium homodimer) cells showed hASCs on all substrates (ELP-D, scrambled-ELP-D, and non-coated glass) were adherent and alive (with average viabilities of 98.9%±0.5%, 98.8%±0.3%, and 98.4% ±0.7%, respectively). This result was expected, as ASCs are known to non-specifically adhere to many surfaces such as non-coated glass at longer time points. This cell adhesion is presumably due to the presence of ASC-secreted matrix proteins as well as serum proteins in the medium, which can adsorb to the substrate and induce cell adhesion. Additionally, quantification of cell metabolism using an alamarBlue® assay found cells on all substrates to be similarly metabolically active at the six-day time point (Fig. S3).

These results validate the use of photo-processed ELP-D as a biomaterial, as it can elicit specific cell-matrix interactions and is cytocompatible. The increased adhesion rate of hASCs on ELP-D versus scrambled-ELP-D films at early time points confirms that the RGD domain retains its cell-adhesive functionality even after photo-processing. As expected, at longer time points, hASC adhesion to the protein thin films is no longer dependent on RGD-cell interactions. This is presumably due to the non-specific adsorption of serum-rich medium components onto the film as well as the secretion of extracellular matrix proteins by the hASCs. The increased adhesion rate of hASCs on ELP-D thin films, even in a serum-rich environment, is promising for applications in which rapid cell adhesion is desired.

## Conclusions

In this study, we demonstrated the successful functionalization of a bioactive, recombinantly engineered elastin-like protein with a photoactive moiety to enable the versatile photo-processing of stable, cell-adhesive biomaterials. The extensive processing versatility of ELP-D was demonstrated through the fabrication of both two- and three-dimensional biomaterials using a variety of techniques including spin coating, drop casting, soft lithographic patterning, and mold casting followed by crosslinking via ultraviolet light exposure. ELP-D spin coated thin films were shown to be highly stable for up to three weeks, making them an attractive option for potential biomaterial coating and drug delivery applications. Finally, we validated the specific cell-adhesive properties of ELP-D as compared to non-coated and scrambled-ELP-D controls, showing that the engineered bioactive functionality of the RGD domain remained active post-processing and crosslinking. A highly clinically relevant cell type, primary human adipocyte-derived stem cells, adhered more rapidly and with larger spread cell area to the ELP-D surfaces compared to controls. The surfaces were highly cytocompatible and maintained cell metabolism for up to six days. These data suggest that ELP-D biomaterials are well suited for future applications as tissue engineering scaffolds for regenerative medicine therapies. The scalability of ELP recombinant production and photo-functionalization to synthesize ELP-D, coupled with the wide range of processing possibilities, high stability, cytocompatibility,

and modular bioactivity make this material a promising choice for further development for a wide variety of biomedical applications.

## Supplementary Material

Refer to Web version on PubMed Central for supplementary material.

## Acknowledgments

The authors acknowledge funding from NSF DMR-0846363, NIH R21-AR-062359, NIH DP2-OD-006477 and a National Science Foundation Graduate Fellowship (A.P.-A). The authors thank Lydia-Marie Joubert and Bob Jones for assistance with SEM, Adam Sturlaugson for use of FTIR, and Reinhold Dauskardt and Krysta Biniek for assistance with mechanical tests.

## References

1. Ciardelli G, Chiono V. Macromolecular bioscience. 2006; 6(1):13–26. [PubMed: 16374766]
2. Datta, Nh; Holtorf, HL.; Sikavitsas, VI.; Jansen, JA.; Mikos, AG. Biomaterials. 2005; 26(9):971–977. [PubMed: 15369685]
3. de Mel A, Jell G, Stevens MM, Seifalian AM. Biomacromolecules. 2008; 9(11):2969–2979. [PubMed: 18831592]
4. Rammelt S, Schulze E, Bernhardt R, Hanisch U, Scharnweber D, Worch H, Zwipp H, Biewener A. Journal of Orthopaedic Research. 2004; 22(5):1025–1034. [PubMed: 15304275]
5. Linnola RJ, Sund M, Ylonen R, Pihlajaniemi T. Journal of Cataract and Refractive Surgery. 1999; 25(11):1486–1491. [PubMed: 10569163]
6. Bossi S, Benvenuto A, Wieringa P, Di Pino G, Guglielmelli E, Boretius T, Stieglitz T, Navarro X, Micera S. Conference proceedings : ... Annual International Conference of the IEEE Engineering in Medicine and Biology Society. IEEE Engineering in Medicine and Biology Society. Conference. 2010; 2010:1527–1530. [PubMed: 21096373]
7. Bumgardner JD, Wiser R, Gerard PD, Bergin P, Chestnutt B, Marini M, Ramsey V, Elder SH, Gilbert JA. Journal of Biomaterials Science-Polymer Edition. 2003; 14(5):423–438. [PubMed: 12807145]
8. Babensee JE, Anderson JM, McIntire LV, Mikos AG. Advanced Drug Delivery Reviews. 1998; 33:111–139. (1,Äì2). [PubMed: 10837656]
9. Tibbitt MW, Anseth KS. Biotechnology and Bioengineering. 2009; 103(4):655–663. [PubMed: 19472329]
10. Banta S, Wheeldon IR, Blenner M. Annual Review of Biomedical Engineering, Vol 12. 2010; 12:167–186.
11. Romano NH, Sengupta D, Chung C, Heilshorn SC. Biochimica Et Biophysica Acta-General Subjects. 2011; 1810(3):339–349.
12. Krishna OD, Kiick KL. Biopolymers. 2010; 94(1):32–48. [PubMed: 20091878]
13. Liu Y, Liu B, Riesberg JJ, Shen W. Macromolecular bioscience. 2011; 11(10):1325–1330. [PubMed: 21830299]
14. Straley KS, Heilshorn SC. Soft Matter. 2009; 5(1):114–124.
15. Liu JC, Tirrell DA. Biomacromolecules. 2008; 9(11):2984–2988. [PubMed: 18826275]
16. Cappello J, Crissman J, Dorman M, Mikolajczak M, Textor G, Marquet M, Ferrari F. Biotechnology progress. 1990; 6(3):198–202. [PubMed: 1366613]
17. Lutolf MP, Tirelli N, Cerritelli S, Cavalli L, Hubbell JA. Bioconjugate Chemistry. 2001; 12(6): 1051–1056. [PubMed: 11716699]
18. Grieshaber SE, Farran AJE, Lin-Gibson S, Kiick KL, Jia XQ. Macromolecules. 2009; 42(7):2532–2541. [PubMed: 19763157]
19. Liu S, Maheshwari R, Kiick KL. Macromolecules. 2009; 42(1):3–13. [PubMed: 21494423]
20. Nowatzki PJ, Tirrell DA. Biomaterials. 2004; 25(7–8):1261–1267. [PubMed: 14643600]

21. Lim DW, Nettles DL, Setton LA, Chilkoti A. Biomacromolecules. 2007; 8(5):1463–1470. [PubMed: 17411091]
22. Di Zio K, Tirrell DA. Macromolecules. 2003; 36(5):1553–1558.
23. Nie Z, Kumacheva E. Nature materials. 2008; 7(4):277–290.
24. Nguyen KT, West JL. Biomaterials. 2002; 23(22):4307–4314. [PubMed: 12219820]
25. Benson RS. Nuclear Instruments and Methods in Physics Research Section B: Beam Interactions with Materials and Atoms. 2002; 191:752–757. (1,Äì4).
26. Decker C. Macromolecular Rapid Communications. 2002; 23(18):1067–1093.
27. Anderson DG, Tweedie CA, Hossain N, Navarro SM, Brey DM, Van Vliet KJ, Langer R, Burdick JA. Advanced Materials. 2006; 18(19) 2614-+
28. Chin JW, Martin AB, King DS, Wang L, Schultz PG. Proceedings of the National Academy of Sciences of the United States of America. 2002; 99(17):11020–11024. [PubMed: 12154230]
29. Carrico IS, Maskarinec SA, Heilshorn SC, Mock ML, Liu JC, Nowatzki PJ, Franck C, Ravichandran G, Tirrell DA. Journal of the American Chemical Society. 2007; 129(16):4874-+. [PubMed: 17397163]
30. Wang S, Wong Po Foo C, Warrier A, Poo MM, Heilshorn SC, Zhang X. Biomedical microdevices. 2009
31. Coin I. Journal of Peptide Science. 2010; 16(5):223–230. [PubMed: 20401924]
32. Tang Y, Tirrell DA. Journal of the American Chemical Society. 2001; 123(44):11089–11090. [PubMed: 11686725]
33. Sun N, Panetta NJ, Gupta DM, Wilson KD, Lee A, Jia F, Hu S, Cherry AM, Robbins RC, Longaker MT, Wu JC. Proceedings of the National Academy of Sciences of the United States of America. 2009; 106(37):15720–15725. [PubMed: 19805220]
34. Zuk PA, Zhu M, Ashjian P, De Ugarte DA, Huang JI, Mizuno H, Alfonso ZC, Fraser JK, Benhaim P, Hedrick MH. Molecular Biology of the Cell. 2002; 13(12):4279–4295. [PubMed: 12475952]
35. Bunnell BA, Flaat M, Gagliardi C, Patel B, Ripoll C. Methods. 2008; 45(2):115–120. [PubMed: 18593609]
36. Urry DW. Journal of Physical Chemistry B. 1997; 101(51):11007–11028.
37. Chow DC, Dreher MR, Trabbic-Carlson K, Chilkoti A. Biotechnology progress. 2006; 22(3):638–646. [PubMed: 16739944]
38. Sigrist H, Muhlemann M, Dolder M. Journal of Photochemistry and Photobiology B-Biology. 1990; 7(2–4):277–287.
39. Gambi A, Winnewisser M, Christiansen JJ. Journal of Molecular Spectroscopy. 1983; 98(2):413–424.
40. Kramer W, Schneider S. Journal of Lipid Research. 1989; 30(8):1281–1288. [PubMed: 2769079]
41. Huang Z, Daniels RH, Enzerink RJ, Hardev V, Sahi V, Goodman SB. Tissue engineering. Part A. 2008; 14(11):1853–1859. [PubMed: 18950272]
42. Kim W, Chaikof EL. Advanced Drug Delivery Reviews. 2010; 62(15):1468–1478. [PubMed: 20441783]
43. Williams C, Brown XQ, Bartolak-Suki E, Ma HW, Chilkoti A, Wong JY. Biomaterials. 2011; 32(2):410–418. [PubMed: 20858564]
44. Badie N, Bursac N. Biophysical Journal. 2009; 96(9):3873–3885. [PubMed: 19413993]
45. Mecham RP, Broekelmann TJ, Fliszar CJ, Shapiro SD, Welgus HG, Senior RM. The Journal of biological chemistry. 1997; 272(29):18071–18076. [PubMed: 9218437]

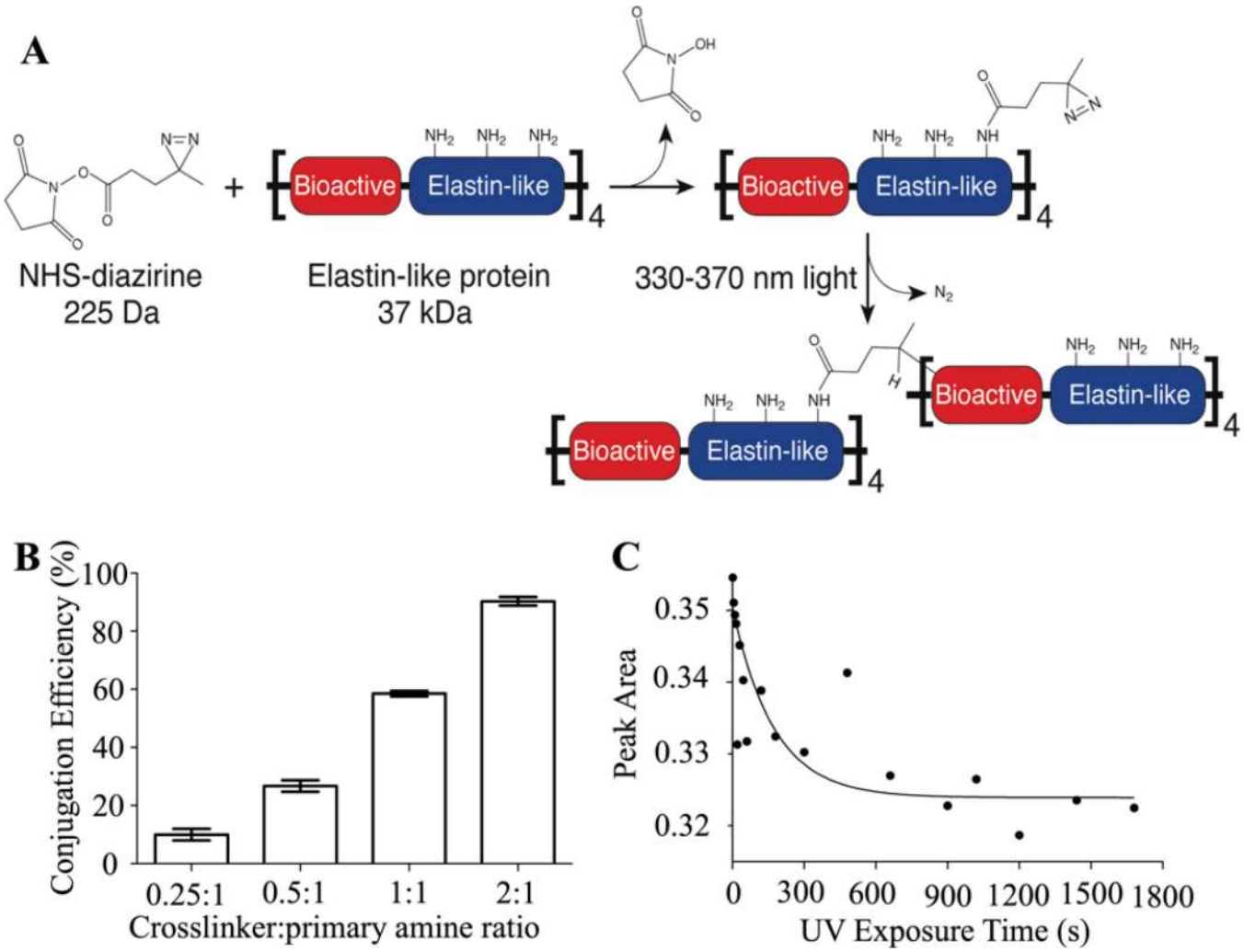


**Fig. 1.**

Conjugation of a photoreactive diazirine group to an engineered ELP. (A) Schematic of crosslinker conjugation chemistry. Primary amines within ELP (present at the N-terminus and on side chains of lysine residues) react with the NHS-diazirine crosslinker to form an amide bond, thereby synthesizing a diazirine-modified ELP (ELP-D). Upon exposure to ultraviolet light, the diazirine group forms a highly reactive carbene intermediate, which can insert into a neighboring ELP chain. (B) Conjugation efficiency as a function of crosslinker:primary amines stoichiometry. (C) FTIR data of characteristic diazirine peak (1460 $cm^{-1}$) first-order exponential decay as a function of UV exposure time, with $t_{1/2}$ = 119 seconds.

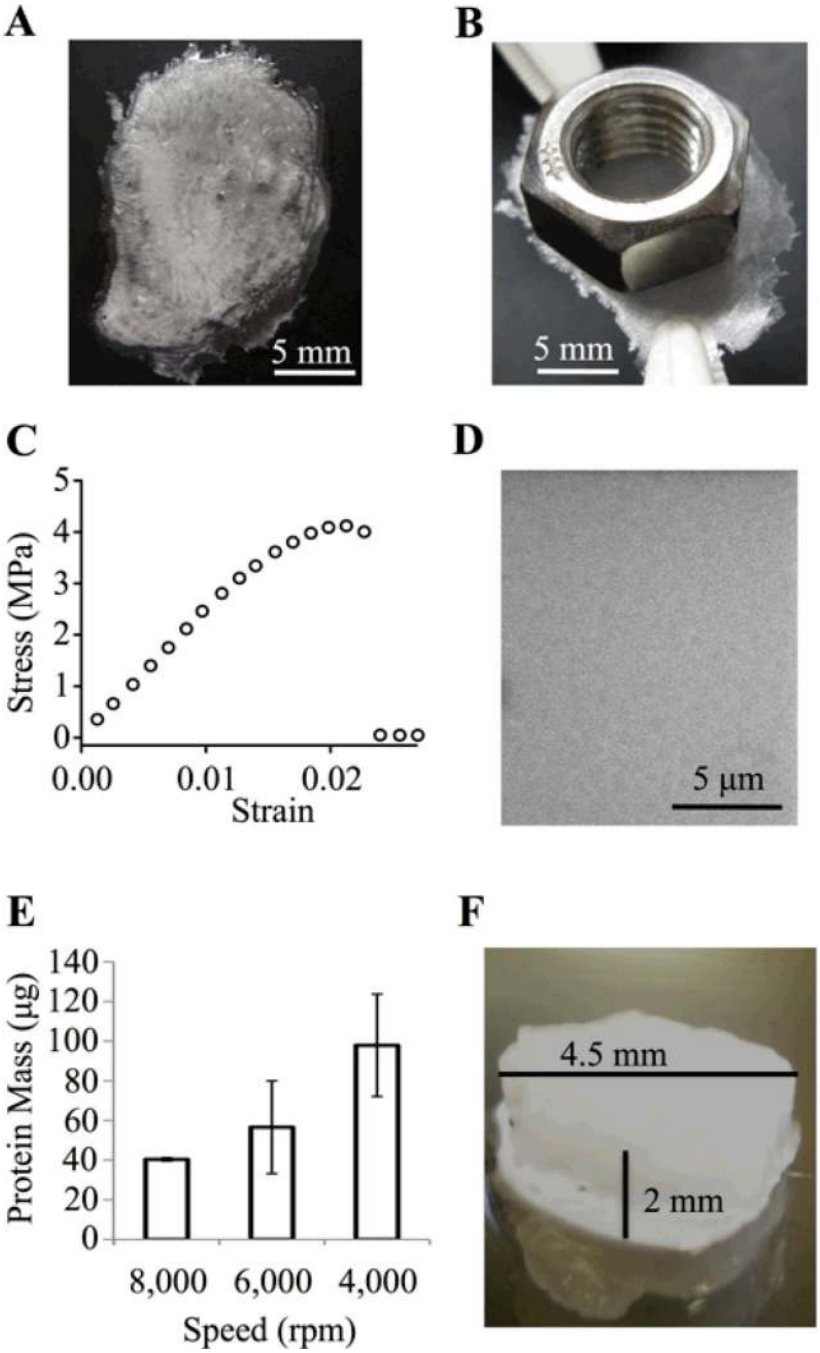


**Fig. 2.**

Versatile photo-processing of ELP-D materials. (A) Drop cast, free-standing ELP-D film (t~50 μm), which (B) has sufficient strength to hold a 4.5 g mass. (C) Tensile stress-strain curve for ELP-D drop cast film, Young's modulus ~250 MPa. (D) SEM image of spin coated photocrosslinked ELP-D thin film (t~500 nm) showing uniform protein coverage. (E) Protein mass of thin films is controlled by processing at specific spin coating speeds. (F) Bulk, three-dimensional ELP-D scaffold (t~2 mm, d~4.5 mm).

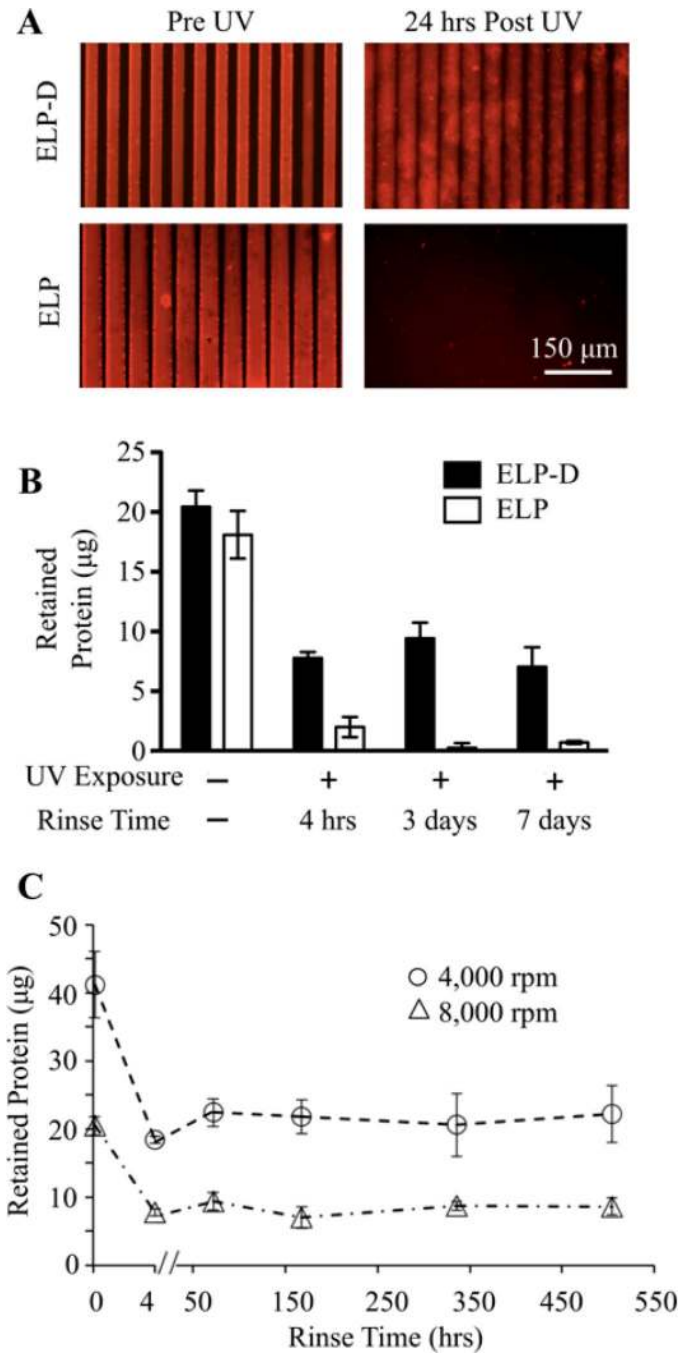


**Fig.3.**

Photocrosslinked ELP-D stability. (A) Fluorescent images of ELP-D (top) and ELP (bottom) scaffolds micropatterned by soft lithography to have a repetitive striped topography (50 μm wide, 5 μm depth pattern). Dried scaffolds prior to UV light exposure clearly shows the presence of topography (left), while 24 hours after UV exposure and rinsing, only the hydrated ELP-D scaffold remains. (B) Mass of protein retained in spin coated thin films prior to UV exposure and at various times post exposure (in solution), for ELP and ELP-D samples. (C) Long-term, hydrated stability of spin coated ELP-D thin films processed to have different initial masses.

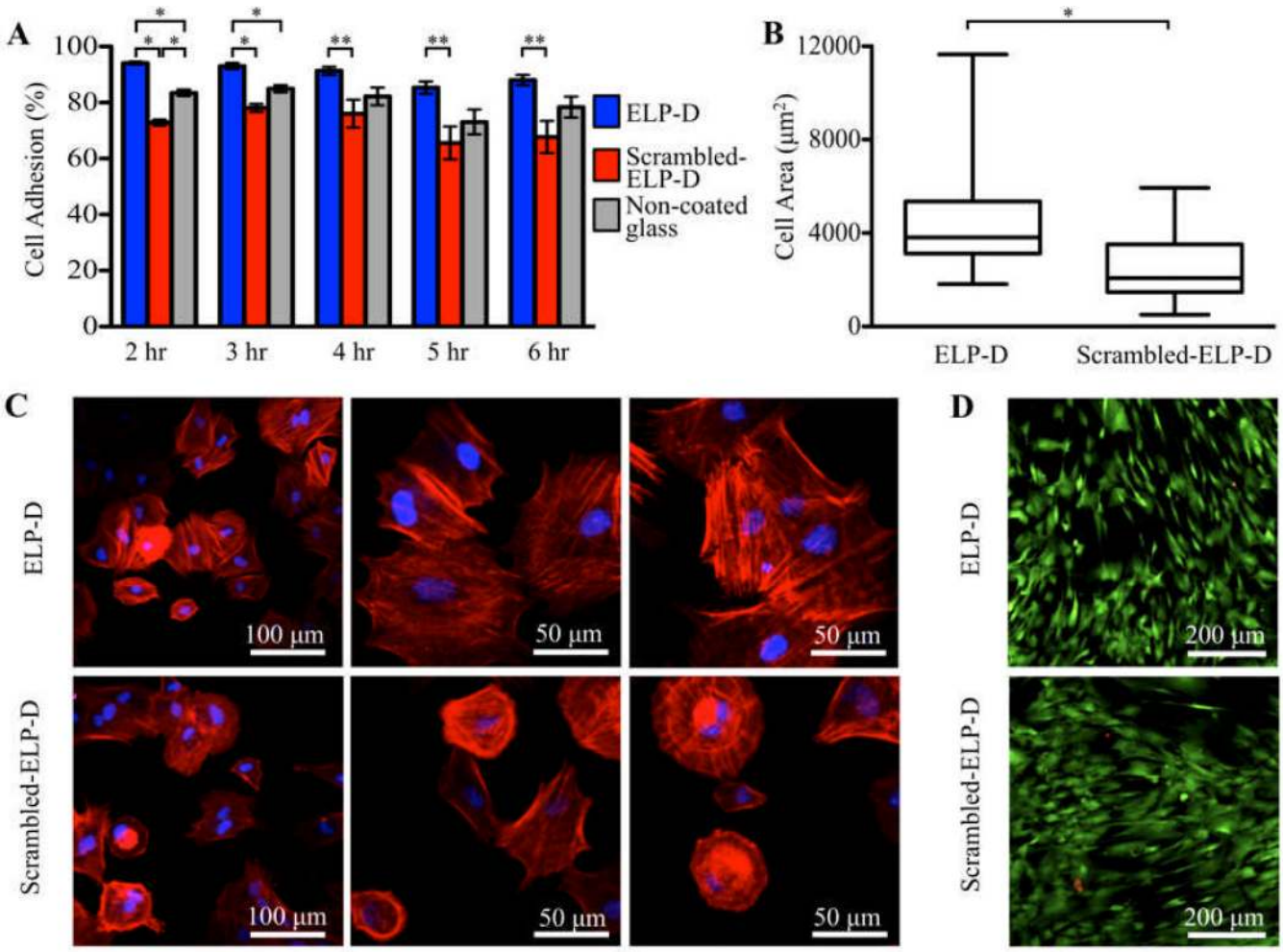


**Fig.4.**

Culture of hASC on ELP-D thin films. (A) Percentage of adherent hASC to ELP-D (which contains a cell-adhesive RGD sequence), scramble-ELP-D (negative control), and non-coated glass coverslips. (* $p < 0.0001$, ** $p < 0.02$) (B) hASC spread area on ELP-D and scramble-ELP-D thin films at 4 hours. Data shown as a box-and-whisker plot; bottom and top of the box mark the 25$^{th}$ and 75$^{th}$ percentiles, respectively; horizontal band in the box marks the median, and whiskers mark the 5$^{th}$ and 95$^{th}$ percentiles. (* $p < 0.001$) (C) Representative hASC morphology on ELP-D (top) and ELP (bottom) thin films at 4 hours after fluorescent staining staining of nuclei (DAPI, blue) and F-actin (phalloidin, red). (D) Day 6 fluorescent staining of live (calcein AM, green) and dead (ethidium homodimer, red) hASCs on ELP-D and scramble-ELP-D thin films demonstrating long-term viability of cells on ELP materials.